# Electronic Supplementary Information (ESI)

## A new self-desalting solar evaporation system based on vertically oriented porous polyacrylonitrile films

Qian Zhang[a,b†], Hongjun Yang[b†], Xingfang Xiao[b], Han Wang[b], Zhuoxun Shi[a], Lei Yan[a], Yali Chen[b], Weilin Xu[*,b], and Xianbao Wang[*,a]

a. Hubei Collaborative Innovation Center for Advanced Organic Chemical Materials, Key Laboratory for the Green Preparation and Application of Functional Materials, Ministry of Education, Hubei Key Laboratory of Polymer Materials, School of Materials Science and Engineering, Hubei University, Wuhan 430062, P. R. China

b. State Key Laboratory of New Textile Materials & Advanced Processing Technologies and Hubei Key Laboratory of Advanced Textile Materials & Application, Wuhan Textile University, Wuhan 430200, P. R. China

† These authors contributed equally to this work.

*Corresponding author Email: weilin_xu0@163.com,wangxb68@aliyun.com

### ESI Methods of material characterization

The morphologies of samples were observed using a feld-emission scanning electron microscope (FESEM; Sigma 500, Zeiss, Germany). Samples were characterized by Fourier transform infrared (FT-IR) spectroscopy (iS50, Nicolet, USA). X-ray photoelectron spectroscopy (XPS) was carried out on an XP spectrometer (ESCALAB 250Xi, Thermo Fisher Scientific, USA). The Raman spectra were obtained using a confocal Raman spectrometer (inVia, Renishaw, UK) at an excitation wavelength of 532 nm. The absorption performance was measured in the wavelength range of 200 to 2500 nm using an ultraviolet–visible spectrophotometer (Lambda 950, PerkinElmer, USA) equipped with an integration sphere. The integrating sphere was used to collect the scattered light for accurate measurements. The air permeability of samples was measured with an air permeability tester (G321, Gellowen Science, UK) through a given area (5 $cm^2$) of the fabric at a given pressure (100 MPa). The mechanical properties of cotton fabrics were measured using a materials

testing machine (Model 5566, Instron, USA) at a strain rate of 20 mm $min^{-1}$. For each measurement, five samples were tested and the mean value was used. The durability of the RGO/cotton fabric to washing was carried out according to the Chinese standard GB/T 12490-2007. A standard color-fast washing machine (Model SW-LZA, Changzhou Dahua Electronic Instrument Co., Ltd., China) was used to launder the fabric. The RGO/cotton fabric (5×5 cm) was washed at 50 °C for 30 min in a rotating closed canister containing 150 mL of aqueous detergent solution (4 g $L^{-1}$); the above is considered as one washing cycle. A computer color-matching system (Color i7; X-Rite, USA) was used to measure the *K*/*S* value of the RGO/cotton fabric after washing.

**ESI Solar-powered steam generation**

The solar-powered steam generation experiments were conducted in the ambient temperature of ~25 °C with the humidity of ~55%. A solar simulator (a xenon lamp, CELHXF300, Education Au-light Co Beijing, China) was used to supply simulated sunlight, and a calibrated power meter (CEL-NP2000, Education Au-light Co Beijing, China) measure incoming radiative flux. In this work, the incoming radiative flux was measured over 5 distributed locations and averaged. All samples were irradiated by a solar simulator with a light density of 1 kW $m^{-2}$ (1 sun=1 kW $m^{-2}$) for 60 min at a steady state condition. During irradiation, the mass change of water in the beaker was recorded by an electronic balance(Sartorius, SQP, QUINTIX224-1CN）with an accuracy of 0.0001 g. Moreover, the beaker was wrapped in polyurethane foam (thickness: 26 mm) as a heat-insulating wall to reduce thermal loss. To confirm the reusability of the system, the steam generation process of RGO/cotton fabric was measured by recording the mass change as a function of time, and the evaporation examination was repeated 16 times under the same conditions. For each cycle, RGO/cotton fabric was irradiated under one sun. After 60 min, the wetted RGO/cotton fabric was dried and re-arranged for the next cycle.

**ESI-Video S1 to Video S7**

**ESI-Fig. S1 to Fig. S28**

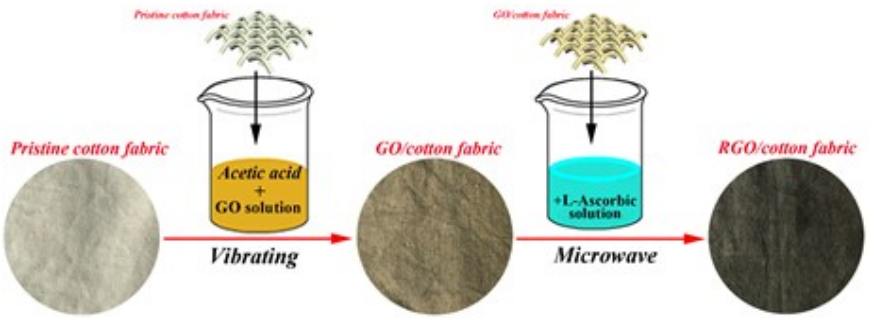


**Fig. S1.** Fabrication process of RGO/cotton fabric.

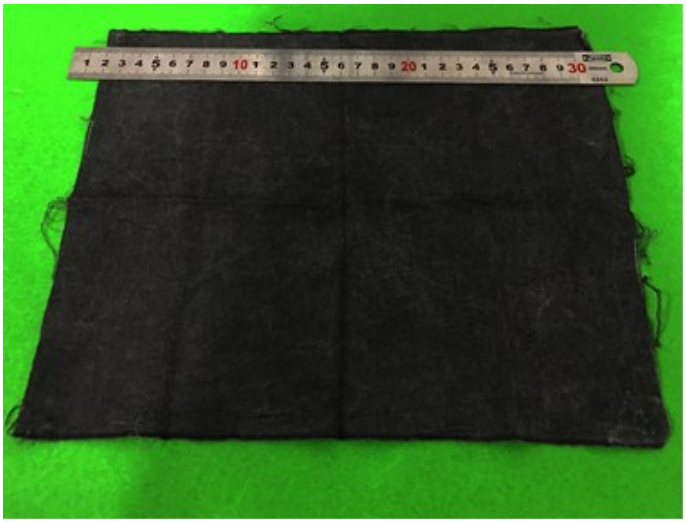

**Fig. S2.** Larger-sized RGO/cotton fabric.

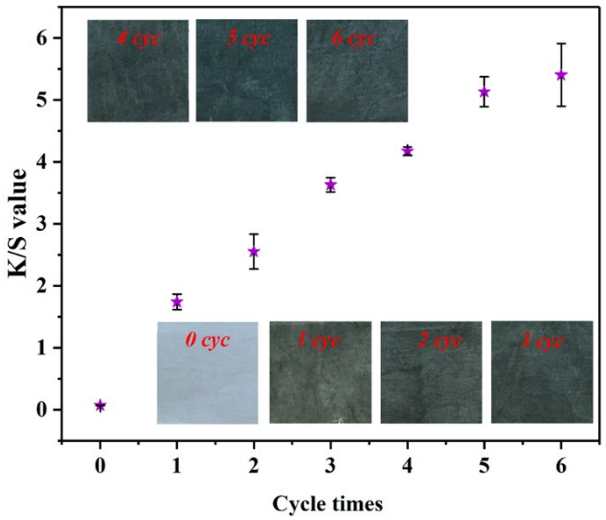


**Fig. S3.** *K*/*S* value of the RGO/cotton fabric as functions of number of treated cycles (0 cycle presents pristine cotton fabric). Insert: the coresponding optical image of RGO/cotton fabric.

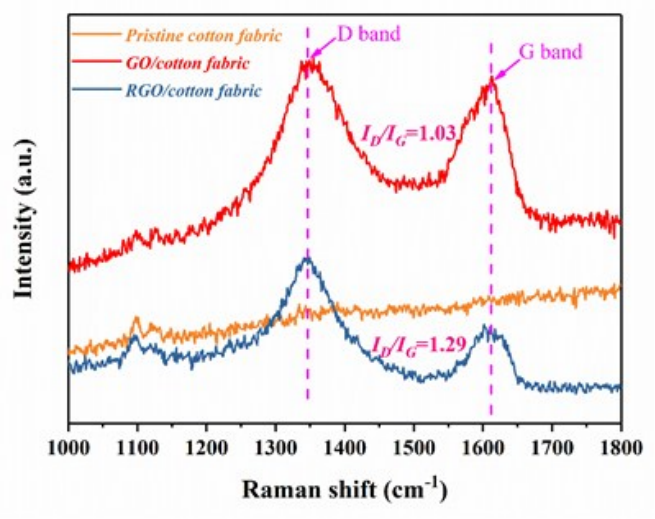


**Fig. S4.** Raman spectra of pristine cotton fabric, GO/cotton fabric, and RGO/cotton fabric, obtained with an excitation wavelength of 532 nm.

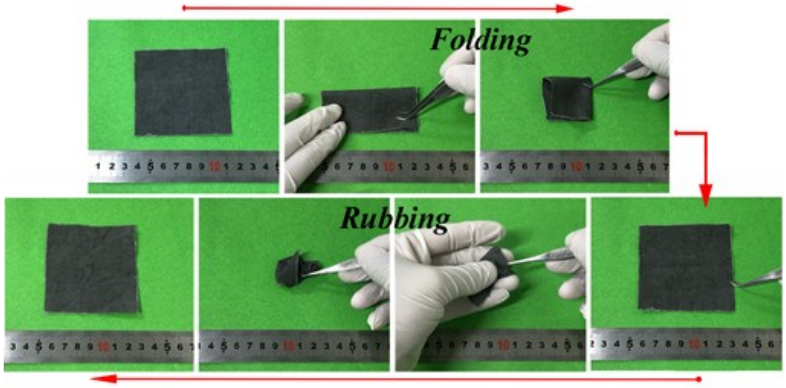


**Fig. S5.** Photographs of RGO/cotton fabric with high flexibility.

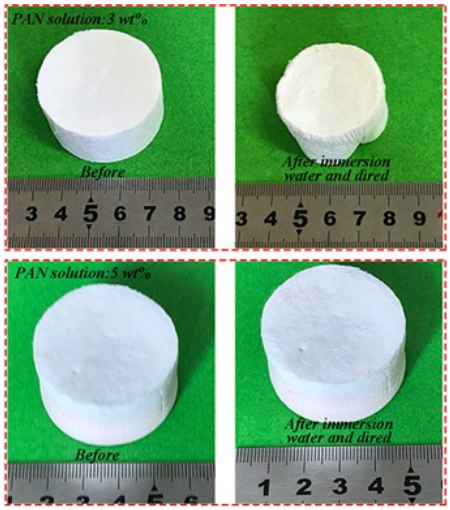


**Fig. S6.** Optical image comparision of VOPPF (PAN soultion, 3 wt% and 5 wt%) after immersion water and dried.

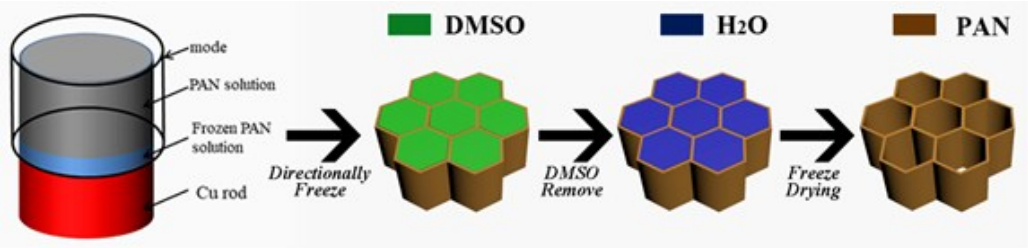


**Fig. S7.** Fabrication process of VOPPF.

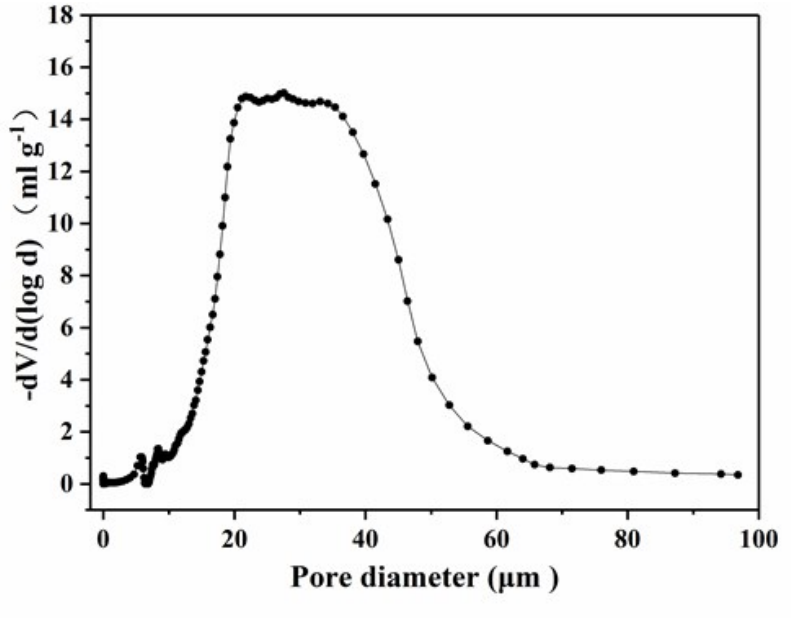


**Fig. S8.** Pore size distribution of VOPPF as measured by Hg intrusion porosimetry.

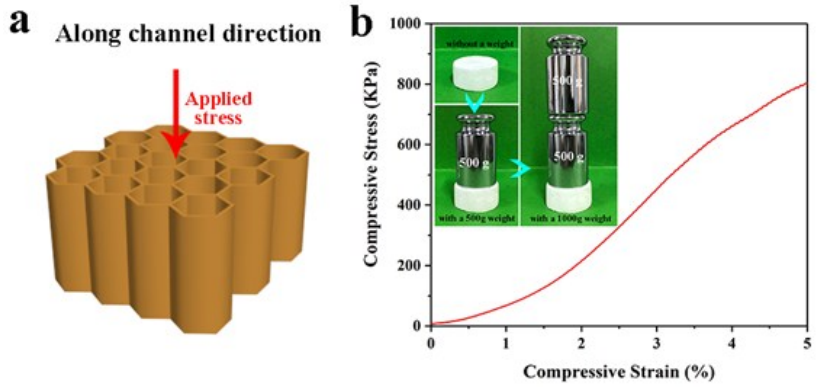


**Fig. S9.** (a) Schematic of the loading direction along channel direction. (b) Typical compressive σ–ε curves for VOPPF (ε = 5%) tested along channel direction. Insert image: VOPPF-5 showing its mechanical robustness that can support a 500 g and 1000 g weight without compressive deformation along channel direction.

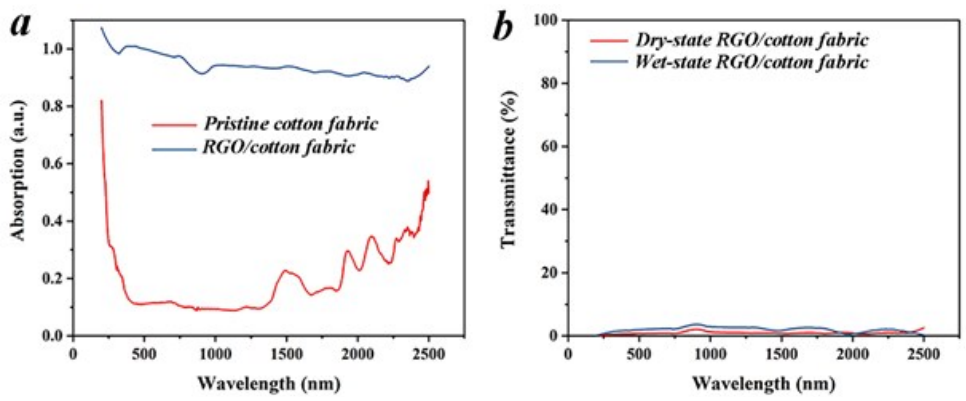


**Fig. S10.** (a) Absorbance comparison between pristine cotton fabric and RGO/cotton fabric. (b) Transmittance spectra of RGO/cotton fabric (both dry-state and wet-state) in the wavelength range of 200~2500 nm.

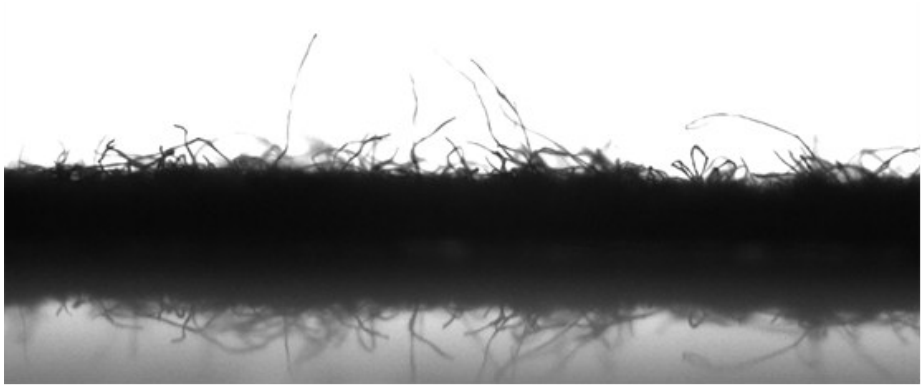

**Fig. S11.** Side-view of RGO/cotton fabric by camera.

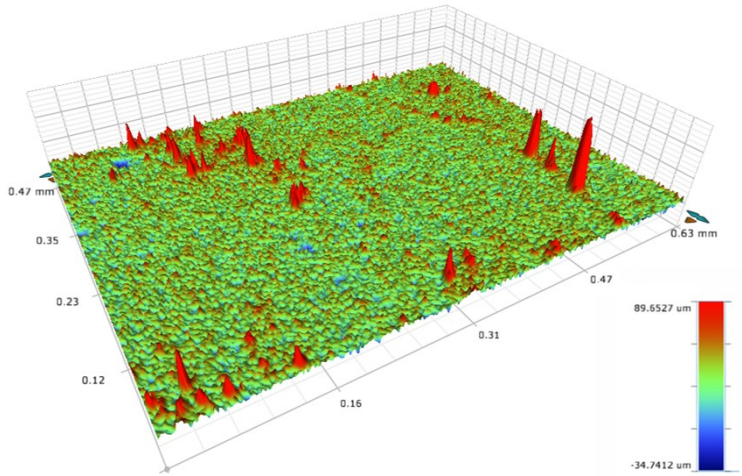


**Fig. S12.** 3D optical image of RGO/cotton fabric.

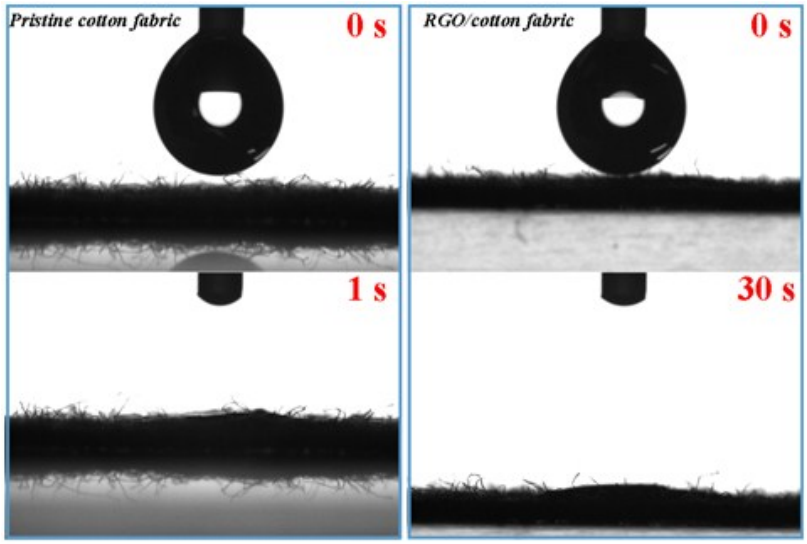


**Fig. S13.** Dynamic wetting of water droplet (3 μL) on pristine cotton fabric and RGO/cotton fabric.

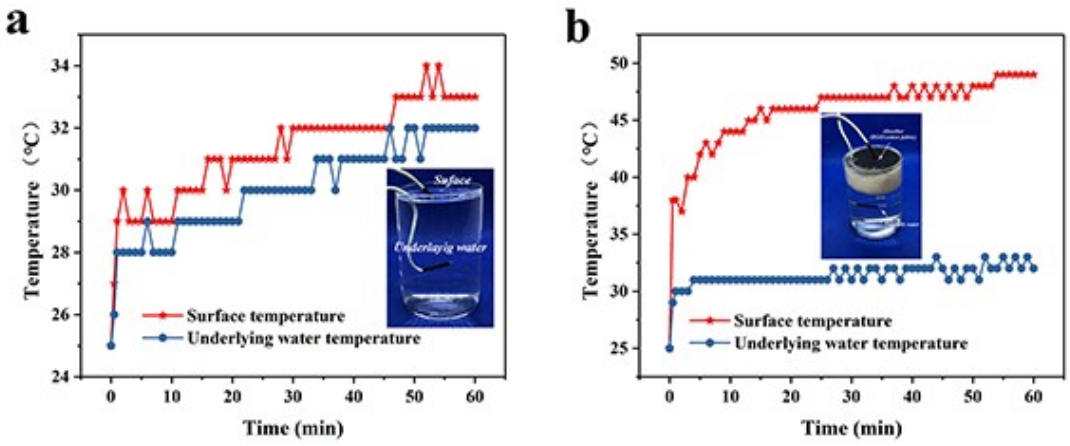


**Fig. S14.** (a) water only and (b) water with RGO/cotton fabric + VOPPF under one sun illumination in surface and underlying water (Inserts show the measurement position).

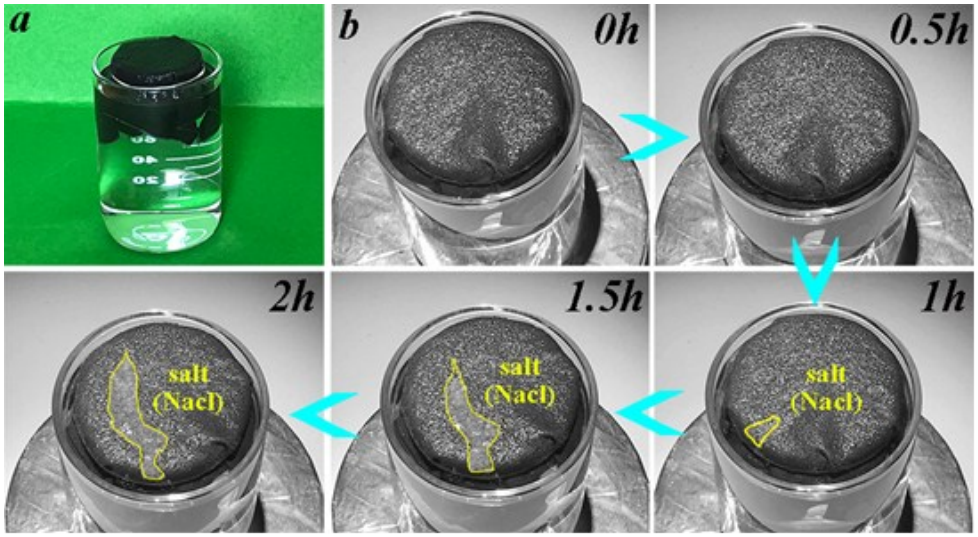


**Fig. S15.** (a) Optical image of 2D water channel solar steam generator based on RGO/cotton fabric. (B) Progression of salt precipitation on the surface of RGO/cotton fabric under one sun.


**Fig. S16.** Optical images of the bulk saturated NaCl solution. The recrystallized salts are not found in saturated NaCl solution, when the extra salt on the upper of evaporator fully disappeared.

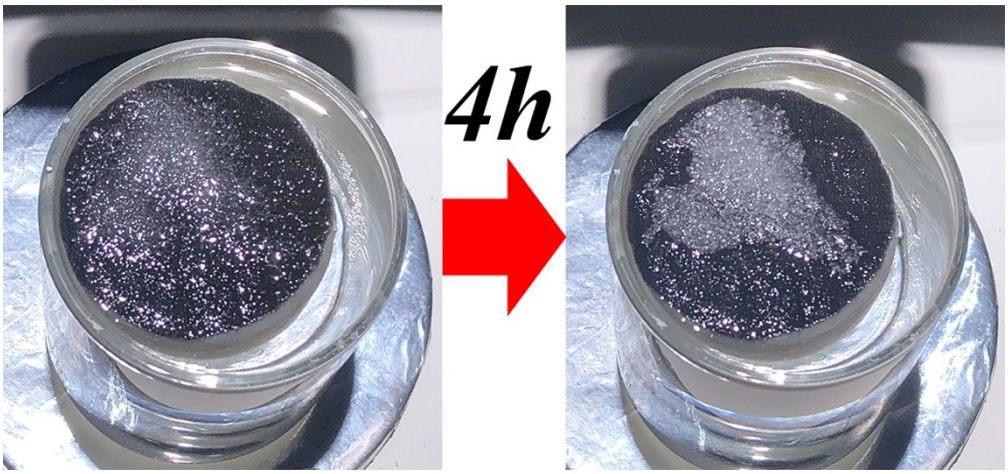


**Fig. S17.** Progression of salt rejection under one-sun illumination in the evaporation system placed into saturated NaCl solution, when the salt was up to 4 g. The above amount of the extra salt on the upper of evaporator remained on RGO/cotton fabric after 4 h in saturated NaCl solution.

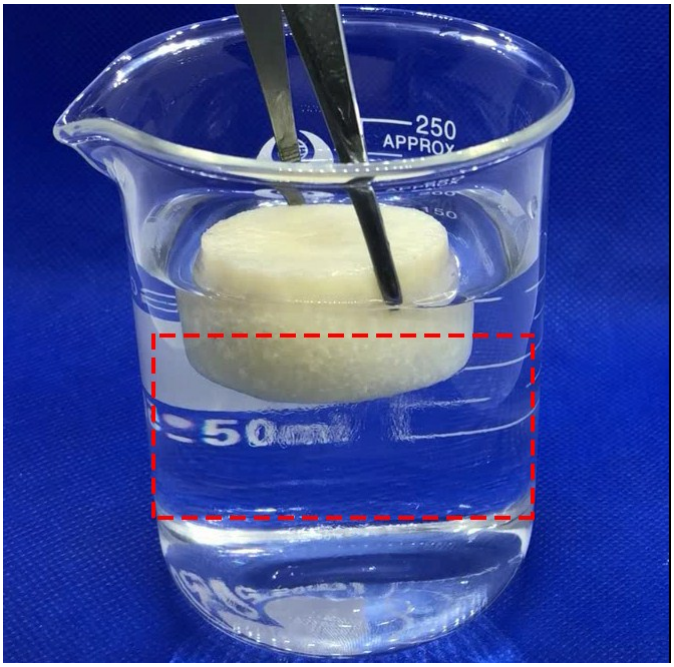


**Fig. S18.** The downward flow of the recrystallized salt solution from VOPPF.

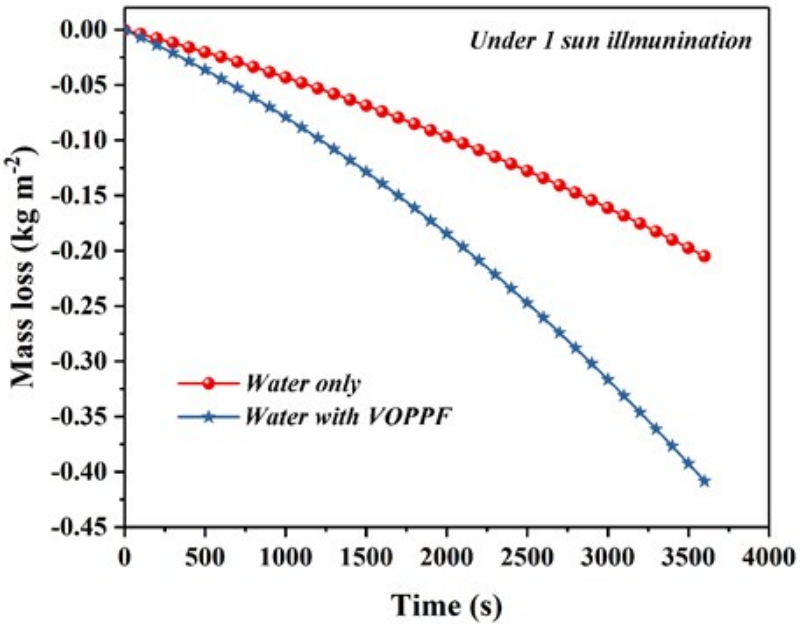


**Fig. S19.** Evaporation mass loss of water only and water with VOPPF under one sun solar irradiation for 60 min.

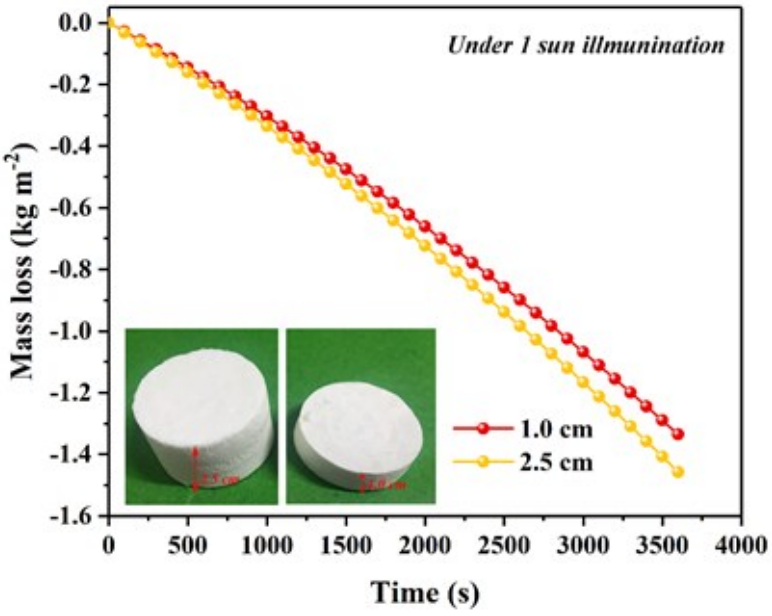


**Fig. S20.** Evaporation mass loss of water with RGO/cotton fabric in presence of VOPPF at various height under one sun solar irradiation for 60 min. Insert image: Optical image of VOPPF with various height.

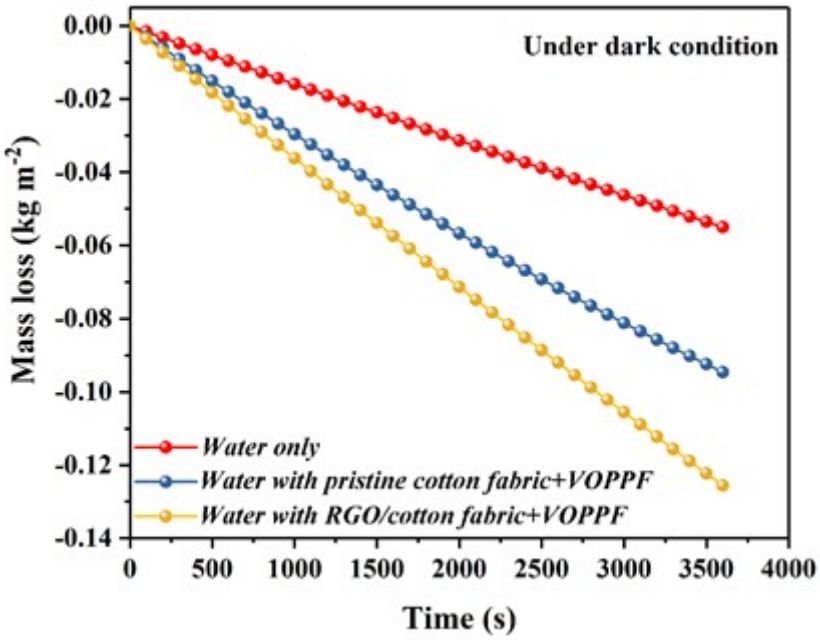


**Fig. S21.** Evaporation mass loss of water only, water with pristine cotton fabric+VOPPF and water with RGO/cotton fabric+VOPPF under dark condition for 60 min.

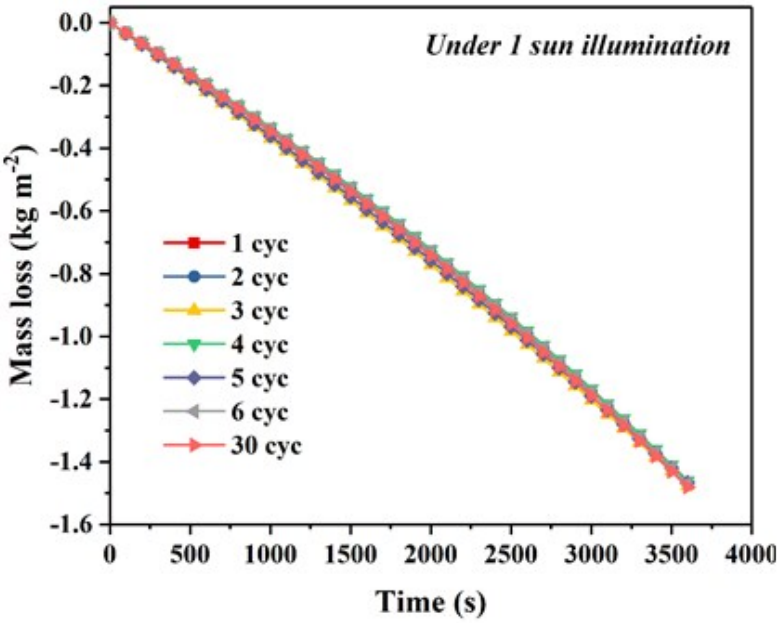


**Fig. S22.** Evaporation mass loss of water upon RGO/cotton fabric +VOPPF as functions of number of washing cycles under one sun illumination for 60 min.

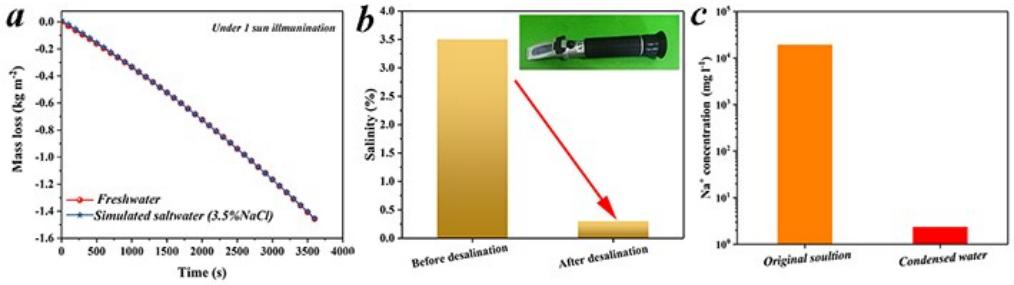


**Fig. S23.** (a) Evaporation mass loss of freshwater, saltwater (3.5wt% NaCl) upon RGO/cotton fabric +VOPPF under one sun illumination for 60 min. (b) The salt concentration comparison before and after desalination (insert image : a refractometer ). (c) Concentrations of Na ion original soultion and condensed water were determinated by inductively coupled plasma–optical emission spectroscopy .

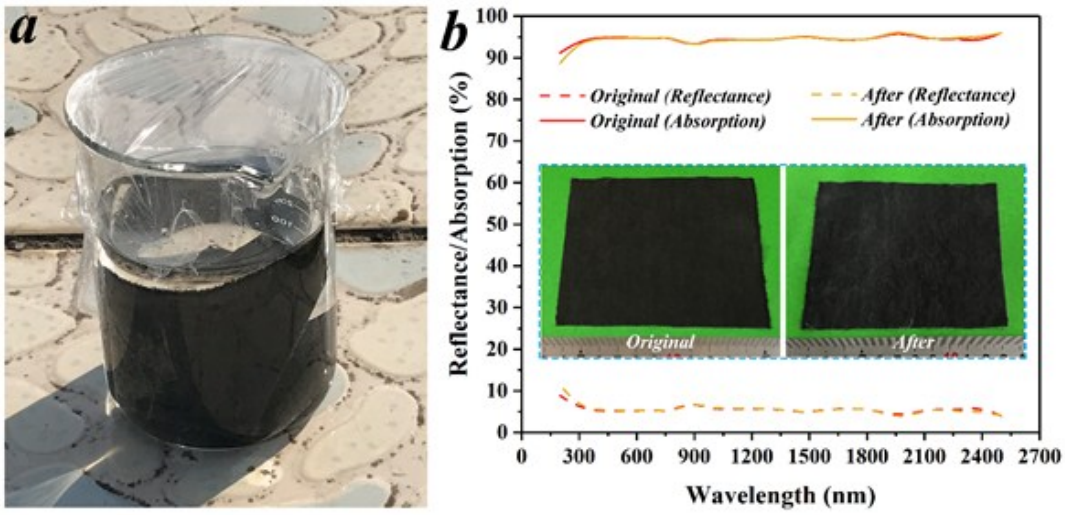


**Fig. S24.** (a) Optical image of RGO/cotton fabric immersed in 3.5% NaCl solution under outdoor environment. (b) The absorption spectra of RGO/cotton fabric before and after 10 days in 3.5% NaCl solution under outdoor environment. (Insets are the photographs of RGO/cotton fabric before and after 10 days in 3.5% NaCl solution under outdoor environment, respectively.)

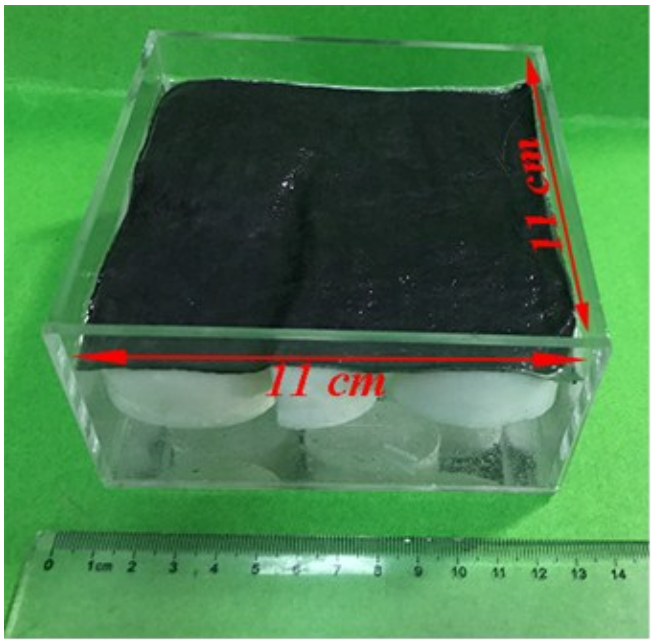


**Fig. S25.** Larger-sacle solar steam generation device consisted of a large scale RGO/cotton fabric (11×11 cm) and several smaller VOPPF.

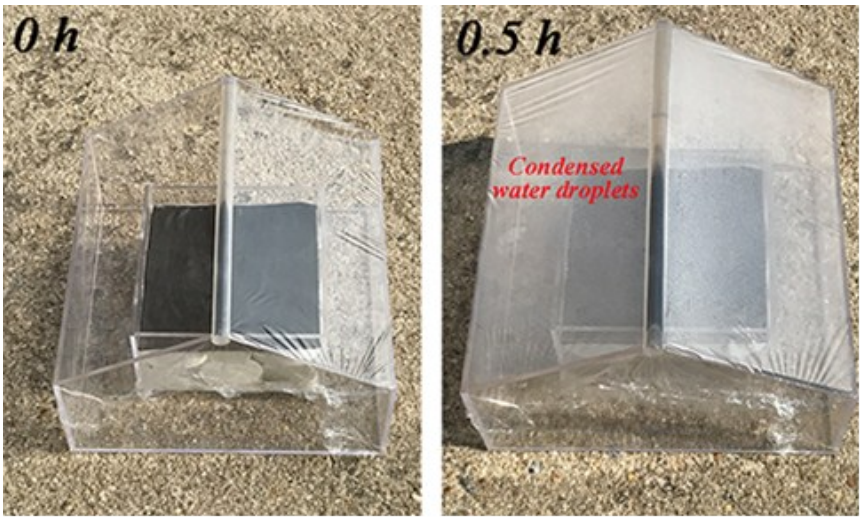


**Fig. S26.** Image of clean water production system based on RGO/cotton fabric and VOPPF working at the outdoor environment.

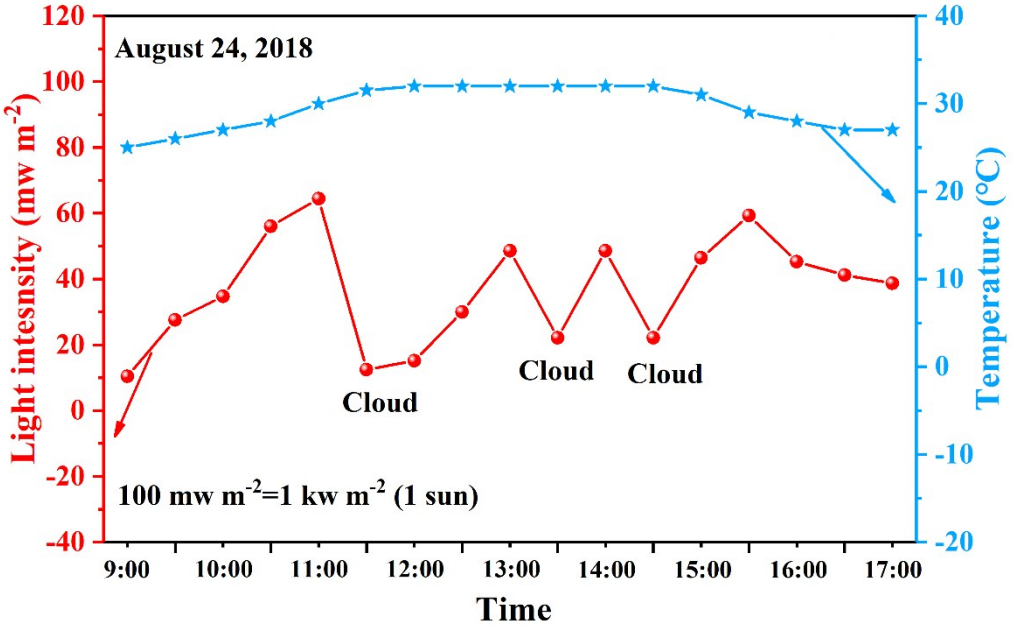


**Fig. S27.** The outdoor solar intensity and temperature variation curves from 9:00 to 17:00 on August 24, 2018 at the campus of Wuhan Textile University, Jiangxia District, Wuhan, China.


**Fig. S28.** The weight change of simulated saltwater before and after desalination under nature solar light.

**The solar steam generation efficiency ($\eta$) was calculated using the following equation:**[1,2]

$$\eta = \dot{m}(h_{LV} + Q)/E_{in}, \quad (1)$$

where $E_{in}$ (kJ $m^{-2}$ $h^{-1}$) is the energy input of the incident light, $\dot{m}$ is the water evaporation rate (kg $m^{-2}$ $h^{-1}$), $h_{LV}$ is the total enthalpy of the liquid water to vapor transition ($h_{LV}$ = 1.918 ×

$10^6$ $[T/(T - 33.91)]^2$ J $kg^{-1}$),[3] $T$ is the temperature of evaporation, and $Q$ is the specific sensible heat of water. In particular, $Q$ can be expressed as $Q = c(T - T_1)$ J $kg^{-1}$, where $c$ is the specific heat capacity of water (4.2 J $g^{-1}$ $K^{-1}$), and $T_1$ is water/air interface.

**The analysis of heat loss.**[4-6]

The heat loss of the solar evaporation device consists of three parts: (1) radiation, (2) convection, and (3) conduction.

(1) Radiation:

The radiation loss was calculated by the Stefan-Boltzmann equation.

$$\Phi=\varepsilon A\sigma(T_1^4-T_2^4) \quad (1)$$

Where $\Phi$ represents heat flux, ε is the emissivity, and emissivity in this equation is supposed has a maximum emissivity of 0.97. A (3.14*4 $cm^{-2}$) is the surface area, $\sigma$ is the Stefan-Boltzmann constant, $T_1$ is the average surface temperature of absorber at a steady state condition, and $T_2$ is the ambient temperature upward the absorber. Under the illumination of constant solar flux (1 sun). The radiation heat loss is calculated to be ~2.8%

(2) Convection:

The convective heat loss is defined by Newton' law of cooling.

$$Q= hA\Delta T \quad (2)$$

Where $Q$ represents the heat energy, h is the convection heat transfer coefficient, which is about 5 W $m^{-2}$ K as reported,[7] and $\Delta T$ is different value between the average surface temperature of srGA and the ambient temperature upward the absorber. The connection heat loss is calculated to be ~2%

(3) Conduction:

$$Q=Cm\Delta T \quad (3)$$

Where $Q$ is the heat energy, $C$ is the specific heat capacity of water (4.2 kJ $^oC^{-1}$ $kg^{-1}$), m is the weight of pure water (10 g) used in this experiment. $\Delta T$ is the average temperature difference of pure water after and before solar illumination under 1 sun after 1 h. The conduction heat loss is calculated to be ~4.6%

References

1. Xiuqiang, L.; Renxing, L.; George, N.; Ning, X.; Xiaozhen, H.; Bin, Z.; Guangxin, L.; Jinlei, L.; Shining, Z.; Jia, Z., Natl. Sci. Rev. 2018, 5, 70-77.
2. Y. Yang, H. Zhao, Z. Yin, J. Zhao, X. Yin, N. Li, D. Yin, Y. Li, B. Lei, Y. Du and W. Que, *Mater. Horiz.*, 2018, **5**, 1143-1150.
3. Henderson-Sellers, B., Q. *J. R. Meteorol. Soc.*, 1984, **110**, 1186-1190.
4. Y.J. Li, T.T. Gao, Z. Yang, C.J. Chen, W. Luo, J.W. Song, E. Hitz, C. Jia, Y.B. Zhou, B.Y. Liu, B. Yang, L.B. Hu, *Adv. Mater*., 2017, **29**, 1700981.
5. N. Xu, X.Z. Hu, W.C. Xu, X.Q. Li, L. Zhou, S.N. Zhu, J. Zhu, *Adv. Mater.*, 2017, **29**, 1606762.
6. G. Ni, G. Li, S.V. Boriskina, H.X. Li, W.L. Yang, T.J. Zhang, G. Chen, *Nat. Energy*, 2016, **1**, 16126–16132.
7. H. Ghasemi, G. Ni, A.M. Marconnet, J. Loomis, S. Yerci, N. Miljkovic, G. Chen, *Nat. Commun.*, 2014, **5,** 5449–5455.